Progress in single-biomolecule analysis with solid-state nanopores

Albrecht, T.

DOI:
10.1016/j.coelec.2017.09.022

Document Version
Peer reviewed version

Citation for published version (Harvard):
Albrecht, T 2017, 'Progress in single-biomolecule analysis with solid-state nanopores', *Current Opinion in Electrochemistry*, vol. 4, no. 1, pp. 159-165. https://doi.org/10.1016/j.coelec.2017.09.022

Progress in Single-Biomolecule Analysis with Solid-State Nanopores

T. Albrecht

School of Chemistry, University of Birmingham, Edgbaston Campus, Birmingham B15 2TT, UK

t.albrecht@bham.ac.uk

Abstract

Solid-state nanopores and nanopipettes are a new class of stochastic, single-molecule sensors that have now reached a certain degree of maturity. While DNA sequencing has been a major driving force in the field of nanopore sensing since the early 1990s, a feat that has now been achieved with modified biological pores, new potential applications emerge, in particular for solid-state devices. These capitalize on some of the advantages of solid-state pores over their biological counterparts as well as recent technological advances and progress in our fundamental understanding of the translocation process. Here, we will discuss and highlight some of these developments with particular focus on single-molecule analysis of and structures based on double-stranded DNA.

Keywords: nanopore sensing; nanopipettes; DNA; fingerprinting; gene profiling

Introduction

Nanopore devices are a new class of stochastic single-molecule sensors. Inspired by small, pore-forming biological channels on one hand and their micrometer-scale analogue, the famous Coulter counter on the other, the field was initially strongly motivated by developing a fast and label-free DNA sequencing technology.[1,2,3,4] After approximately 30 years from its inception, this impressive feat has now been achieved, based on carefully designed biological pores (α-hemolysin). However,

the field has a lot more to offer and new platforms, as well as new applications are now coming into focus. This includes 'solid-state' nanopore sensors, which broadly fall into two categories, *viz*. chip-based nanopores and nanopipettes.[5,6,7] In comparison to biological channels, those pores tend to be somewhat larger and less reproducible. On the other hand they offer more design flexibility and may be more readily be adapted to different and larger analytes, such as protein/DNA complexes.

Generally, the ability of nanopore sensors to detect individual transport events of biological molecules through the pore channel ('translocations'), either electrically or optically, enables the technique to go beyond ensemble-averaged measurements.5,6,[8,9,10,11,12] As will be seen below, they are also capable of resolving sub-structure in large translocating biomolecules, such as knots in double-stranded (ds) DNA, DNA-bound proteins and other features, and modifications, such single-nucleotide polymorphism (SNP), cf. fig. 1.[13,14,15,16,17,18,19,20,21,22,23,24,25] This is an exciting area, which takes advantage of the full information content of the nanopore data and sets it apart from more conventional, ensemble-based characterisation techniques, such as gel electrophoresis and flow cytometry. It has seen significant progress in recent years and is thus the focus of this short review. We will briefly discuss the main challenges involved, based on simple theoretical considerations, revisit the main developments and conclude with a brief outlook.

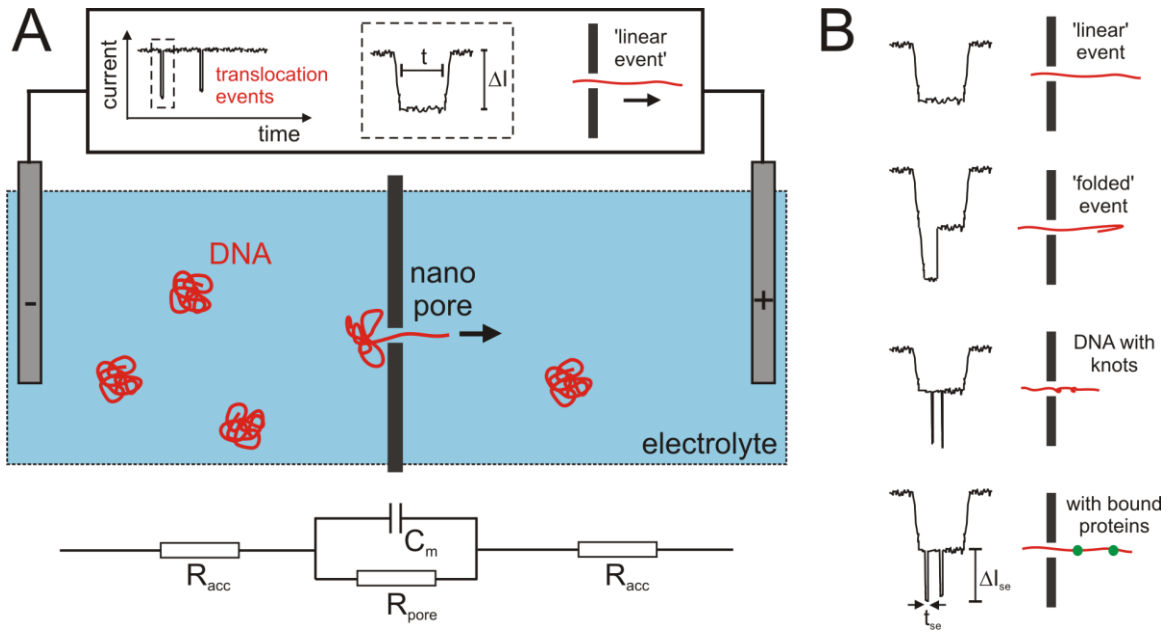

Figure 1: A) Basic nanopore setup with the (black) insulating membrane separating two electrolyte-filled compartments, and the nanopore. A current-induced electric field may be applied via a bias voltage V_{bias} between the electrodes and be used to pull charged analytes, such as DNA (red), through the pore channel. The pore diameter d is typically smaller than 20 nm, the channel length L on the order of 50 nm or shorter. Top: Illustration of the readout signal, namely the current-time trace, with individual DNA translocation events. The blow-up illustrates some key parameters of the event, such as the event duration t and magnitude ΔI. For DNA, a 'rectangular' event shape typically implies that the molecular translocated in a linear configuration. Bottom: A simple equivalent circuit representation with access and pore resistances, R_{acc} and R_{pore}, as well as a membrane capacitance C_m. B) Examples of different event shapes and their relation to the translocating analyte: Linear and folded DNA, as well as DNA with additional structural features, such as knots and bound biomolecules (top to bottom). The complexity and information content of each event increases accordingly.

Fundamental aspects of the DNA translocation process

In most nanopore sensing experiments, the translocation of DNA is driven by a current-induced electric field (electrophoresis), that is in turn the result of a bias, V_{bias}, applied between the two electrodes in the cell, fig. 1. If the resistance of the pore with diameter d and length L is large compared to the solution (or 'access') resistance, then the potential drop across the pore channel is $\Delta\Phi_p \approx V_{bias}$ and the local electric field $E \approx V_{bias}/L$, say roughly 0.1 V/0.05 µm = 2 V/µm. This approximation is more accurate for long and narrow pores (d<<L), but less so for pores in very thin

membranes (such as single-layer graphene).[26,27,28] In those cases, the access resistance can even become dominant and the electric field in the pore channel accordingly weaker. The bulk solution is effectively field-free (Brownian motion dominates), but as *E* gets stronger towards the pore entrance (the field lines converge), there is typically some distance from the pore entrance, the 'capture radius', where the electrophoretic force becomes dominant.[31] Thermal fluctuations are nevertheless always present and can have various effects on the translocation process and, ultimately, the sensor performance. For example, they can cause entering DNA to leave the pore again, against the direction of the electric field, in particular if the latter is small. For large *E*, the drift speed *v* of the DNA is given by the Smoluchovski limit, namely $v = \mu_{el} \cdot E$, where μ_{el} is the electrophoretic mobility. We note that μ_{el} should be regarded as an effective quantity, in that *E* predominantly acts on the polymer segment inside the pore channel and that it becomes inhomogeneous on the outside of the pore.

The translocation process of long dsDNA further warrants some consideration. 'long' here means that the contour length of the DNA, L_{DNA} , is large compared to *L*, and also that $L_{DNA} > L_p$, L_p being the DNA persistence length (~35 nm depending on the electrolyte concentration).[29,30] These conditions are normally met for dsDNA with several 100 base pairs and certainly true in the kbp range. Accordingly, one would expect the DNA to be approximately globular in solution, with a diameter much larger than *d*. Once a DNA molecule gets to within the capture radius, it is pulled towards the pore entrance, where it has to unravel to pass through the pore. This threading process comes at an entropic cost and there is typically an activation barrier associated with pore entry. Hence, one can distinguish barrier-limited translocation for very small pores, where the flux is characterised by an exponential dependence on V_{bias} (very small pores), from flux-limited translocation, which features a linear V_{bias} dependence.[31] The speed of the DNA during the process is determined by electrophoresis and hydrodynamic friction, in some cases potentially also involving surface adsorption effects.[32,33,34]

For sensing purposes not just the average properties of the translocation signal, such as the mean translocation time ‹*t*› or the mean current modulation ΔI, are relevant, but equally the corresponding distributions. It is illustrative to discuss these aspects in a little more detail, inasmuch they inform experimental design and sensor operation.

As pointed out by Ling and Ling,[35] for sufficiently high *E* the translocation time distribution *P*(*t*) may be obtained from Schrödinger's first-passage-time theory, eq. (1):

$$P(t) = \frac{L_{DNA}}{\sqrt{4\pi D t^3}} \cdot e^{-\frac{(L_{DNA}-vt)^2}{4Dt}} \quad (1)$$

where *D* is an effective diffusion coefficient related approximately to the section of DNA that is under the influence of the electric field (inside the pore).

The distribution is in principle asymmetric, depending on *v*, L_{DNA} and *D*, as shown in fig. 2. Its first moment is equal to the mean translocation time, ‹*t*› = L_{DNA}/v, the second moment gives the mean squared translocation time, $\langle t^2 \rangle = \left(\frac{L_{DNA}}{v}\right)^2 + \frac{2DL_{DNA}}{v^3}$.35 Its mode can be shown to occur at $t_{mode} = \frac{\sqrt{(3D)^2+(vL_{DNA})^2}-3D}{v^2}$.

Hence, if $D << vL_{DNA}$, then t_{mode} = ‹*t*›, and the distribution is symmetric: for 10 kbp DNA with realistic parameter values as an example, L_{DNA} = 3400 nm, *v* = 10 nm/μs and *D* = 11.5 $nm^2/\mu s$,35 this yields ‹*t*› = 340 μs and t_{mode} = 339.7 μs. On the other hand, if the parameters were such that $3D = vL_{DNA}$, then $t_{mode} \approx 0.414 \cdot L_{DNA}/v$ = 141 μs, and the asymmetry would be rather significant.

The relative width of the distribution also depends on *v*, L_{DNA} and *D*. With the variance given by $\langle t^2 \rangle - \langle t \rangle^2 = \frac{2DL_{DNA}}{v^3}$, the ratio r_σ between the standard deviation σ and the mean of the distribution (i.e., the relative standard deviation) is equal to $\sqrt{\frac{2D}{vL_{DNA}}}$. For the first numerical example above, this yields r_σ = 2.6% (σ = 8.84 μs; full-width-at-half-maximum (FWHM) = 21 μs). For comparison, if indeed $D = vL_{DNA}/3$ as in the second example above, r_σ would be as large as 81.6% with a FWHM = 271 μs!

Experimentally, the width of the translocation time distribution is found to be even larger, e.g., for 10 kbp DNA closer to 30-40%, in both nanopore chip devices as well as nanopipettes.[33,36] This has been rationalized by local variations in the electroosmotic flow[35] or different structural configurations of the DNA prior to translocation.[36]

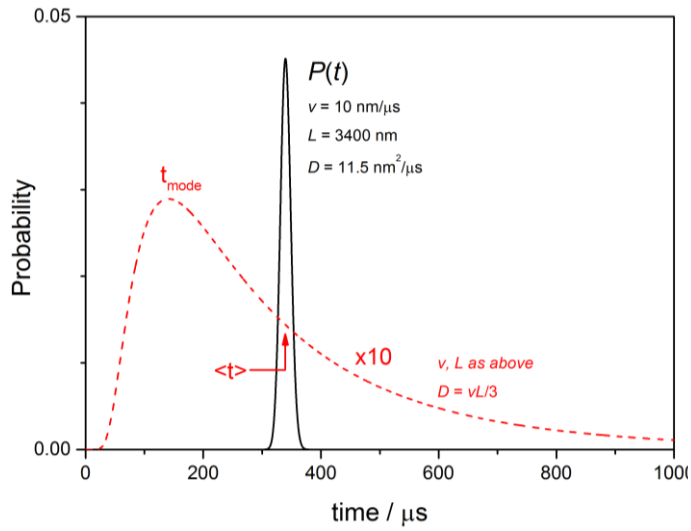

Figure 2: Simulated translocation time distributions according to eq. (1), with parameters as indicated. The probability values for the red distribution (dashed line) are scaled by a factor of 10. Note that both distributions are normalised to 1 and have the same mean translocation time ‹*t*› = 340 μs, while the variance is very different.

It is thus clear from the above considerations that a single observation will not provide a very accurate characterisation of the translocating DNA, at least not based on the translocation time alone. However, the theoretical relative standard deviation r_σ of the distribution, obtained above for 10 kbp DNA, is comparable to values observed with conventional fragment sizing and fingerprinting techniques, such as pulsed-field gel electrophoresis and flow cytometry (on the order of 2-3%).[37] So once the experimentally observed, additional broadening is further reduced, nanopore sensing might be competitive in this context, especially in light of other advantages, such as the extremely low sample volumes required when coupled to microfluidics.[38]

The statistical considerations around eq. (1) however provide further insight into the capabilities of a nanopore sensor, namely their ability to detect structural features of or biomolecules bound to the DNA. Ling and Ling argue that, in order for two features on the DNA to be temporally resolved (provided that $L << L_{DNA}$), the time difference between them should be equal to or larger than the standard deviation of the translocation time, $\delta t \geq \sqrt{\frac{2DL_{DNA}}{v^3}}$. If the translocation speed v is approximately constant during an event, this translates into a change in location along the DNA of $\delta L_{DNA} = v \cdot \delta t = \sqrt{\frac{2DL}{v}}$ or $\delta L_{DNA} \approx 90$ nm for the 10 kbp DNA example above. With L_{DNA} = 3400 nm, this formally corresponds to approximately 37 features, even though in reality additional broadening and practical limitations will presumably reduce this number somewhat.

Important developments in device design and in low-current, high-bandwidth electronics

Apart from diffusional broadening, the relatively low currents, combined with the high-bandwidth requirement pose an additional challenge. For example, current modulations ΔI are typically in the region of 100(s) pA, depending on the pore dimensions, the applied bias voltage, the solution composition and the analyte. Resolving translocation events for 10 kbp DNA as such is relatively straightforward and at $\langle t \rangle$ = 340 μs may only require a bandwidth of 10 kHz or so.

The situation is however different when trying to detect bound proteins or other structural features along the DNA. As an example, we take an antibody of characteristic length $L_{ab} \approx 10$ nm, causing an additional 'sub-event' current spike of height ΔI_{se}, on top of the event current ΔI, say with $\Delta I_{se} \approx \Delta I$ (cf. fig. 1). If the pore channel is L = 50 nm and average speed of the DNA v = 10 nm/μs as above, then the sub-event duration is approximately $t_{se} \approx$ 60 nm/10 nm/μs ≈ 6 μs. In order to fully resolve such a spike (i.e., without significant filter convolution or aliasing), the sampling time should be at least an order of magnitude greater and the bandwidth of the measurement be in the region of 1 MHz or better (for a more detailed discussion of noise, sampling and filtering in nanopore

experiments, see reference 39). Given the low event amplitudes, this is a formidable challenge and only in recent years such performance has been realized on the basis of new electronics designs, for chip-based nanopores and nanopipettes.[40,41,42] In the latter case, the electronics design involves splitting of the nanopore current into 'DC' and 'AC' channels, where the former contains the 'open pore' background current, while the latter captures all fast modulations, including the translocation events. This has advantages in minimizing high-frequency electric noise, but as a side effect also largely removes the need for background correction and hence facilitates fully automated data processing and analysis.

Detecting local features on DNA

Experimental studies systematically probing structural features along dsDNA in solid-state nanopores date back to about 2009.13,14,[15,16,17,18,19,20,21,22,23,24] As illustrated in fig. 1B, the fundamental idea is that such features result in additional 'sub-events', superimposed on the actual DNA translocation event. The magnitude, duration, integral charge, relative position and other statistical properties may then be analysed and used to extract useful, perhaps diagnostic information about the analyte in question. This can include detecting the presence (or absence) of specific binding sites in the DNA or extracting the exact location of binding sites along the DNA. The latter is complicated by the fact that nanopore recordings are usually in the time domain, so direct conversion to a spatial coordinate requires knowledge of *v*.15 In some cases, suitable calibration procedures may suffice to circumvent this problem, depending on the analytical task at hand. Another complication lies in the variance of the translocation time *t*, which often means that sub-events need to be reported relative to the overall event characteristics.

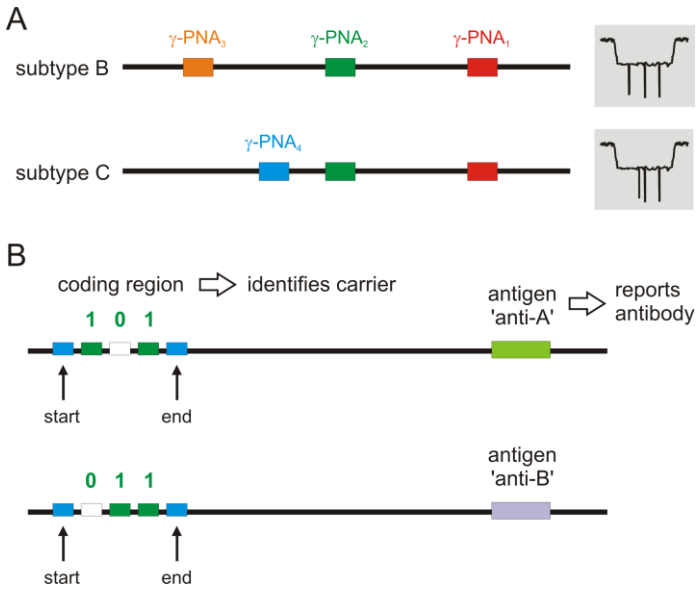

Figure 3: Nanopore-based sensing for gene profiling and fingerprinting applications. A) Two HIV-1 subtypes are distinguished based on the location of the PNA labels: subtype B (binding sites symmetric, labels 1-3; label 4 does not bind) and subtype C (binding sites asymmetric; labels 1,2 and 4; label 3 does not bind).[16] Icons on the right show example translocation events, bearing in mind that the DNA carrier can enter the pore in two orientations. B) Barcoded DNA as an assay for different antibodies.[24] The DNA carrier type is identified via the coding region ('start', 'end' and '1' give sub-event spikes), the antigen-presenting region serves as the site for the respective antibody (additional sub-event spike when bound).

The Meller group was the first to explore the use of short Peptide Nucleic Acids (PNA) for sequence specific binding to dsDNA, towards DNA fingerprinting and profiling applications.15,[16] PNA including some of its synthetic variants can readily bind to duplex DNA with high affinity and locally replace one of the DNA strands upon binding. In the 2012 paper, Meller et al. showed that two 15-mer γ-PNA labels bound to 3 kbp model DNA can be detected (chip-based nanopore, d = 3.7 nm, L = 30 nm, Si_3N_4 membrane), even when the gap between them is as small as 100 bp (~34 nm, *cf.* L). Average translocation times were rather longer than in the example discussed above, with $\langle t \rangle \approx$ 10-20 ms, presumably due to the small pore size. This also facilitated detection of the sub-events. By linear

extrapolation, one might expect $\langle t_{se} \rangle \approx 15/3000 \cdot \langle t \rangle \approx 0.05$-0.1 ms, which could easily be resolved under the conditions used then (50 kHz filter frequency, $\Delta I > 0.35$ nA at a root-mean squared current noise of $I_{rms} \approx 0.05$ nA). In fact, the actual t_{se} was found to be even larger (0.55 $\pm$ 0.06 ms), as the authors suggest either due to the reduced local charge at the PNA binding site or steric interactions between the translocating DNA and the pore itself. In the same work, the authors also demonstrated how a PNA-based binding assay can differentiate between sub-types B and C of the HIV-1 pol gene (~3 kbp, < 8% sequence variance) , fig. 3A. To this end, each sub-type was able to bind three out of four different PNA labels, for convenience named γ-PNA_{1-4}. γ-PNA_{1-3} bound to sub-type B (but not γ-PNA_4), and γ-$PNA_{1,2,4}$ to sub-type C (but not γ-PNA_3). The former resulted in a symmetric binding pattern along the DNA, the latter in an asymmetric one, which was readily identified with the nanopore sensor.

Engineered DNA structures have also been used either as a platform for studying the DNA translocation process itself (DNA velocity and its fluctuations),[23] or as carrier for DNA binding proteins.[43,24] The latter study employed rather sophisticated DNA architectures, inspired by DNA Origami. Specifically, dsDNA was reassembled from long ssDNA and short pieces of ssDNA. The sequences of the latter were chosen, such that the ends were complementary to adjacent parts of carrier, but the central parts were not. As a result, the ends hybridized, while the non-complementary segment remained as a single-stranded loop, protruding from the hybridized carrier. A sufficient number of such loops (~11) formed a group, which could easily be detected by translocation through a nanopipette (inner tip diameter $d \approx 15$ nm), and a total of 5 groups in different places along the DNA carrier served as identifiers for a particular carrier (with a view to probing mixtures), fig. 3B. The first and the last groups were kept the same in all designs, allowing for internal referencing as discussed above, the 3 groups in between were used to identify each carrier ($2^3 = 8$ possibilities). A segment in a different part of the carrier was then modified to include specific binding sites for different antibodies (up to 4 in their case), which would yield an additional

spike when bound. Hence, in a translocation experiment the 3-site barcode allows for the identification of the carrier, the presence (or absence) of an additional spike in the binding region reports on the presence (or absence) of the respective antibody.

This approach has several interesting features. First, conceptually there is seem to be no reason why the number of barcoding sites cannot be increased, say to 4, 5 or even more, providing 16, 32 and more possibilities. The information content of the data could therefore be very high. Secondly, since the event shape is rather distinct, it should be relatively straightforward to differentiate 'true' translocation events from false positives, e.g. other DNA fragments, proteins or other solution species. This should make the methodology more robust in real-life sensing applications, i.e. when coupled to appropriate workflows. Thirdly, the design allows for internal referencing and is tolerant with regards to the orientation of DNA translocation (i.e., which end enters the pore first). A disadvantage could be that each carrier design has to be assembled from small, individual building blocks, which might be expensive, especially when upscaled to larger amounts. All in all, this type of approach appears to be rather promising and opens up new avenues, in terms of different design possibilities, target analytes and so forth.

Conclusions

In a broader context, these two studies illustrate how nanopore and nanopipettes may be employed as stochastic sensor, with clear added value from its single-molecule detection capabilities, compared to ensemble-average methods (e.g., gel electrophoresis). It also becomes clear that the characteristic feature size is on the order of 10s of nm, rather than sub nm - resolving individual bases or base pairs like in a (modified) biological pore is still beyond reach. To this end, it is also debatable, whether it is feasible or indeed desirable to replace the biological components in a nanopore sequencer, given the operational requirements and constraints of the sensor. For

example, an all-solid-state device with a sufficiently thin membrane (to achieve high spatial resolution) and appropriate control over the polymer dynamics (for constant and sufficiently slow translocation speed) might in the end not be more stable or more faster than their biological counterparts.

However, depending on the analytical task at hand, sequencing may not always be needed and the above examples of profiling and fingerprinting, perhaps DNA assaying, offer numerous avenues to be explored in the short- or medium-term. The theoretical basis for such applications is well understood, which allows for strategic design and optimisation of the sensing process (maximising the S/N ratio, minimising the error rates etc.). The focus now shifts towards the context of the nanopore sensor, namely the workflow (sample processing, data handling), robustness of operation and how it compares with competing technologies. As outlined above, there are a number of aspects where nanopore sensors are superior, such as the ability to resolve sub-molecular information and compatibility with ultra-small sample volumes. In how far these have diagnostic value and whether they are offset by other difficulties, remains to be seen. With a view towards a viable sensor technology, further work is clearly required in device fabrication. While small nanopores can be drilled on a wafer scale using focused electron or ion beams,[44] it would presumably be more cost effective to produce pores with suitable geometries in other ways, perhaps based on sacrificial etching. Nanopipettes on the other hand are very easy to make in small numbers employing a pipette puller, even though routine fabrication of pores with single-digit nm diameters has not been demonstrated so far. Unfortunately, the method is not very compatible with mass fabrication and again more efficient methods are desirable in this context.

Taken together, however, progress in nanopore sensing has been rather swift in recent years and many of the inherent challenges have already been solved. Developing a viable and competitive sensing technology is a significant challenge and depends on many factors. From a technological

perspective, nanopore sensing is in many ways still in the early stages, but nevertheless a space to be watched.

References

[1] D Deamer, M Akeson, D Branton, "Three decades of nanopore sequencing", Nat. Biotechnol. 2016, 34, 518-524.
[2] S Carson, M Wanunu, "Challenges in DNA motion control and sequence readout using nanopore devices", Nanotechnology 2015, 26, 074004.
[3] S Agah, M Zheng, M Pasquali, AB Kolomeisky, "DNA sequencing by nanopores: advances and challenges", J. Phys. D: Appl. Phys. 2016, 49, 413001.
[4] F Haque, JH Li, HC Wu, XJ Liang, PX Guo, "Solid-state and biological nanopore for real-time sensing of single chemical and sequencing of DNA", Nano Today 2013, 8, 56-74
[5] J Li, D Stein, C McMullan, D Branton, MJ Aziz, JA Golovchenko, "Ion-beam sculpting at nanometre length scales", Nature 2001, 412, 166-169.
[6] JL Li, M Gershow, D Stein, E Brandin, JA Golovchenko, "DNA molecules and configurations in a solid-state nanopore microscope", Nature 2003, 2, 611-615.
[7] LJ Steinbock, O Otto, C Chimerel, J Gornall, UF Keyser, "Detecting DNA Folding with Nanocapillaries", Nano Lett. 2010, 10, 2493-2497.
[8] GAT Chansin, R Mulero, J Hong, MJ Kim, AJ deMello, JB Edel, "Single-Molecule Spectroscopy Using Nano-porous Membranes", Nano Lett. 2007, 7, 2901-2906.
[9] B McNally, A Singer, Z Yu, Y Sun, Z Weng, A Meller, "Optical Recognition of Converted DNA Nucleotides for Single-Molecule DNA Sequencing Using Nanopore Arrays", Nano Lett. 2010, 10, 2237-2244.
[10] WH Pitchford et al., "Synchronized Optical and Electronic Detection of Biomolecules Using a Low Noise Nanopore Platform", 2015, 9, 1740-1748.
[11] MP Cecchini, A Wiener, VA Turek, H Chon, S Lee, AP Ivanov, DW McComb, J Choo, T Albrecht, SA Maier, JB Edel, "Rapid Ultrasensitive Single Particle Surface-Enhanced Raman Spectroscopy Using Metallic Nanopores", Nano Lett. 2013, 13, 4602-4609.
[12] AP Ivanov, E Instuli, CM McGilvery, G Baldwin, DW McComb, T Albrecht, JB Edel, "DNA Tunneling Detector Embedded in a Nanopore", Nano Lett. 2011, 11, 279-285.
[13] RMM Smeets, SW Kowalczyk, AR Hall, NH Dekker, C Dekker, "Translocation of RecA-coated double-stranded DNA through solid-state nanopores", Nano Lett. 2009, 9, 3089-3096.
[14] M Wanunu, J Sutin, A Meller, "DNA Profilking Using Solid-State Nanopores: Detection of DNA-Binding Molecules", Nano Lett. 2009, 9, 3498-3502.
[15] A Singer, M Wanunu, W Morrison, H Kuhn, M Frank-Kamenetskii, A Meller, "Nanopore Based Sequence Specific Detection of Duplex DNA for Genomic Profiling", Nano Lett. 2010, 10, 738-742.
[16] A Singer, S Rapireddy, DH Ly, A Meller, "Electronic Barcoding of a Viral Gene at the Single-Molecule Level", Nano Lett. 2012, 12, 1722-1728.
[17] D Japrung, A Bahrami, A Nadzeyka, L Peto, S Bauerdick, JB Edel, T Albrecht, "SSB Binding to Single-Stranded DNA Probed Using Solid-State Nanopore Sensors", J. Phys. Chem. B 2014, 118, 11605-11612.
[18] P Nuttall, K Lee, P Ciccarella, M Carminati, G Ferrari, K-B Kim, T Albrecht, "Single-Molecule Studies of Unlabeled Full-Length p53 Protein Binding to DNA", J. Phys. Chem. J. Phys. Chem. B 2016, 120, 2106-2114.
[19] C Plesa, JW Ruitenberg, MJ Witteveen, C Dekker, "Detection of Individual Proteins Bound along DNA Using Solid-State Nanopores", Nano Lett. 2015, 15, 3153-3158.
[20] J Shim et al, "Nanopore-Based Assay for Detection of Methylation in Double-Stranded DNA Fragments", ACS 2015, 9, 290-300.
[21] JS Yu, M-C Lim, DT Ngoc Huynh, H-J Kim, H-M Kim, Y-R Kim, K-B Kim, "Identifying the location of a single protein along the DNA strand using solid-state nanopores" ACS Nano 2015, 9, 5289- 5298.
[22] C Plesa et al., "Direct observation of DNA knots using a solid-state nanopore", Nat. Nanotechnol. 2016, 11, 1093-1098.
* A powerful illustration how nanopore sensing may be used to study the intrinsic, biophysical properties of DNA (here: knotting) in a label-free manner at the single-molecule level.
[23] C Plesa, N van Loo, P Ketterer, H Dietz, C Dekker, "Velocity of DNA during Translocation through a Solid-State Nanopore", Nano Lett. 2015, 15, 732-737.

* This is the first example where engineered DNA structures, i.e. essentially based on DNA Origami, are employed in nanopore sensing. The main focus was to investigate the speed of the DNA during translocation and its variance, and the implications for sensor operation.
[24] NAW Bell, UF Keyser, "Digitally encoded DNA nanostructures for multiplexed, single-molecule protein sensing with nanopores", Nat. Nanotechnol. 2016, 11, 645-652.
** In this paper, Bell and Keyser combine sophisticated DNA design with state-of-the-art detection in quartz nanopipettes. The result is a sensor concept that employs DNA barcoding in a single-molecule antibody assay.
[25] J Kong, J Zhu, UF Keyser, "Single molecule based SNP detection using designed DNA carriers and solid-state nanopores", Chem. Commun. 2017, 53, 436-439.
[26] CA Merchant et al., "DNA Translocation through Graphene Nanopores", Nano Lett. 2010, 10, 2915-2921.
[27] S Garaj, W Hubbard, A Reina, J Kong, D Branton, JA Golovchenko, "Graphene as a subnanometre trans-electrode membrane", Nature 2010, 467, 190-U73.
[28] GF Schneider et al., " DNA Translocation through Graphene Nanopores", Nano Lett. 2010, 10, 3163-3167.
[29] PJ Hagerman, "Flexibility of DNA", Ann. Rev. Biophys. Biophys. Chem. 1988, 17, 265-86.
[30] S Brinkers, HRC Dietrich, FH de Groote, IT Young, B Rieger "The persistence length of double stranded DNA determined using dark field tethered particle motion", J. Chem. Phys. 2009, 130, 215105.
[31] M Wanunu, W Morrison, Y Rabin, AY Grosberg, A Meller, " Electrostatic focusing of unlabelled DNA into nanoscale pores using a salt gradient", Nat. Nanotechnol. 2010, 5, 160-165.
[32] S Ghosal, "Effect of Salt Concentration on the Electrophoretic Speed of a Polyelectrolyte through a Nanopore", Phys. Rev. Lett. 2007, 98, 238104.
[33] M Wanunu, J Sutin, B McNally, A Chow, A Meller, "DNA Translocation Governed by Interactions with Solid-State Nanopores", Biophys. J. 2008, 95, 4 716-4725.
[34] RL Fraccari, P Ciccarella, A Bahrami, M Carminati, G Ferrari, T Albrecht, "High-speed detection of DNA translocation in nanopipettes", Nanoscale 2016, 8, 7604-7611.
* This paper highlights the potential importance of surface effects in DNA translocation, in particular on the scaling behaviour of the translocation time, and its implications for sensor design and operation.
[35] DY Ling, XS Ling, "On the distribution of DNA translocation times in solid-state nanopores: an analysis using Schrödinger's first-passage-time theory", J. Phys.: Condens. Matter 2013, 25, 375102.
[36] B Lu, F Albertorio, DP Hoogerheide, JA Golovchenko, "Origins and Consequences of Velocity Fluctuations during DNA Passage through a Nanopore", Biophys. J. 2001, 101, 70-79.
[37] MM Ferris, X Yan, RC Habbersett, Y Shou, CL Lemanski, JH Jett, TM Yoshida, BL Marrone, "Performance Assessment of DNA Fragment Sizing by High-Sensitivity Flow Cytometry and Pulsed-Field Gel Electrophoresis", J. Clin. Microbiol. 2004, 42, 1965-1976.
[38] TR Gibb, AP Ivanov, JB Edel, T Albrecht, "Single Molecule Ionic Current Sensing in Segmented Flow Microfluidics", Anal. Chem. 2014, 86, 1864-1871.
[39] V Tabard-Cossa, "Instrumentation for Low-Noise High-Bandwidth Nanopore Recording", chapter 3 in "Engineered Nanopores for Bioanalytical Applications", Elsevier 2013 (eds. JB Edel, T Albrecht)
[40] JK Rosenstein, M Wanunu, CA Merchant, M Drndic, KL Shepard, "Integrated nanopore sensing platform with sub-microsecond temporal resolution", Nat. Methods. 2012, 9, 487-492.
[41] S Shekar,DJ Niedzwiecki, C-C Chien, P Ong, DA Fleischer, J Lin, JK Rosenstein, M Drndic, KL Shepard, "Measurement of DNA Translocation Dynamics in a Solid-State Nanopore at 100 ns Temporal Resolution", Nano Lett. 2016, 16, 4483-4489.
** This paper demonstrates how the time resolution in electric nanopore recording may be pushed significantly below the 1 μs mark, by systematically optimizing nanopore device design, high-speed electronics and other factors.
[42] RL Fraccari, M Carminati, G Piantanida, T Leontidou, G Ferrari, T Albrecht, "High-bandwidth detection of short DNA in nanopipettes", Faraday Discuss. 2016, 193, 459-470.
[43] NAW Bell, UF Keyser, "Specific Protein Detection Using Designed DNA Carriers and Nanopores", J. Amer. Chem. Soc. 2015, 137, 2035-2041.
[44] J Klingfus, A Nadzeyka, S Bauerdick, T Albrecht, JB Edel, "Wafer-Scale Ion Beam Lithography of Nanopore Devices", Microsc. Microanal. 2013, 19 (Suppl 2), 912-913.